Cornell University
Department of Biological and Environmental Engineering

Optimization of Conventional pMDIs for a Better Salbutamol Delivery System

2 May 2013

Prepared and Presented by

Ha (Natalie) Luu

Kimberly Lin

Danya Contreras

Stephanie Curley

Table of Contents

1. EXECUTIVE SUMMARY

The most commonly prescribed method of treatment for asthma today is the pressurized metered dose inhaler (pMDI). However, many patients fail to use it correctly, resulting in the inefficient administration of the drug. There are two main methods to maximize the efficacy of an inhaler: 1) increasing the concentration of the drug per dose; and 2) optimizing drug particle deposition in the lungs by minimizing deposition in the upper airway. Previous studies have shown that doubling the inhaled dose is minimally effective, and it also increases the risk of experiencing side effects. Thus, minimizing particle deposition in the upper airway is the more viable approach. Computational fluid dynamics (CFD) modeling is necessary for determining the ideal parameters that will minimize the drug loss during species transfer and maximize the drug's effectiveness. The goal of this study is to develop a model that simulates the particle trajectory and deposition of salbutamol, an anti-asthma drug (Drug Information Online, 2013), through the oral cavity and laryngeal-trachea regions of the upper respiratory tract. Besides modeling the system, topics of optimal flow rate, initial velocity of drug particles at the mouth inlet, and aerosol drug size are also discussed.

The COMSOL Multiphysics 4.3 simulation software was used to solve the governing equations employed in our simulation. Turbulent fluid flow from inhalation was modeled with 2-dimensional Navier Stokes fluid flow equations, and the Lagrangian Particle Tracking method was used to describe the distribution of the drug. Fraction of particle deposition in the upper airway tract was determined for a range of breathing flow rates, inlet particle velocities, insertion angles, and particle sizes to find optimal values. Deposition of salbutamol at different inhaler insertion angles was also measured.

Results showed that particle deposition is minimized with particle diameters of 1-10μm and flow rates of 30-60 L/min. A subtle dependence on particle velocity was noted for particles of 10-20μm in size; there was a small increase in deposition as particle velocity increased for a given flow rate and particle size. For a particle diameter of 30μm, as much as 100% of all particles deposited in the upper airway tract for the higher flow rates of 50, 60, and 75 L/min. For particles that were <10μm, the percentage of particles that deposited in the respiratory tract did not change appreciably with changing particle inlet velocity across all flow rates tested, consistently showing ~3.5% particle deposition. For medium-sized particles that were between 10μm and 30μm in diameter, the amount of drug reaching the lungs can be maximized by choosing a lower flow rate, <50 L/min, and lower spray velocity, <7.3 m/s. For salbutamol in particular, the amount of deposition at different spray cone angles did not show a significant trend.

The implications of our findings will lead future designs of pMDI to focus on obtaining the optimal combination of parameters for drug size, breathing flow rate, and particle inlet velocity. Our observations on the dependence of particle deposition on drug size will allow extending the

application of our model to other drugs of different sizes and potentially lead to modifying inhalers accordingly. For future studies, our analysis can be extended to consider the deposition location for the same range of flow rates, spray velocities, and drug sizes, and spray cone angle. In addition, the effect of different mouth geometries on deposition location can be explored.

Keywords*: inhaler, salbutamol, pMDI, particle deposition, asthma*

2. INTRODUCTION

2.1 **Rationale of the project**

Asthma is a chronic inflammatory disorder of the airways that affects 34 million Americans of all ages (Kay, A. B., et al, 2008 and Asthma Health Center, 2005). This chronic inflammatory disorder is associated with hyperresponsiveness of the airways that leads to recurrent episodes of wheezing, breathlessness, chest tightness, and coughing. In order to prevent serious asthma attacks, patients are recommended to use asthma inhalers to administer drugs. Inhalers have the advantage that they deposit drugs directly to the lungs. This delivery system allows for higher effective drug concentration without increasing the dose, while also minimizing contact with the rest of the body.

One type of inhaler, the Pressurized Metered-dose inhaler (pMDIs), is widely used to deliver aerosolized medication deep into the lungs (Crosland, B. M., et al, 2009). pMDIs are commonly used by patients because of their portability, low airflow resistance, and generation of aerosols independent of inspiratory flow rate (Ehtezazi, T., et al, 2009). Svartengren et al and Ehtezazi et al have done pMDI studies investigating spray particle size, flow rate in the oral cavity, spray injection angle, injection velocity, material properties of the particle, and deposition mechanisms to note how upper airway tract symptoms can be alleviated. Out of these elements studied, we decided to focus on spray injection angle, flow rate, injection velocity and particle size.

In Svartengren et al. (1996), the mouthpiece of the asthma inhaler was increased in order to study the effects on the deposition of 3.5 μm particles in the oropharynx and lungs. It was found that on average there was no significant difference in outcome. So, elongating the mouthpiece is not an efficient solution to the deposition issue. In Ehtezazi et al.(2009), particles smaller than 0.83 μm are independent from the oropharyngeal geometry; therefore ultrafine pMDIs are more favorable.

Studies like these of the post-nozzle flow of aerosol drops for optimization tried lengthening the mouthpiece of pMDIS or increasing the inhaler inflow resistance in order to decrease the oropharyngeal deposition (Svartengren, K., et al, 1996). However, the increase in size was not suitable for patients with an average oropharyngeal deposition. The effect only seemed to be significant to some patients with abnormally high depositions. Also, the increased resistance did not significantly decrease the deposition, since the problem of deposition resides in the oropharyngeal geometry. Consequently, researchers used various imaging techniques to model effects of particle size along with the difference in aerosol delivery between the use of an ultrafine and conventional pDMI, in which ultrafine is with a diameter less than 1 μm. The comparison of delivery methods allowed researchers to see if delivery independent of the oropharyngeal geometry is enabled (Ehtezazi, T., et al, 2009). In Ehtezazi's study, the ultrafine particle was found to be preferable. But this method would require allotting time and space for evaporation of the propellant and cosolvent from the initial aerosol particles to reduce the particle size (Ehtezazi, T., et al, 2009).

Our research focuses on optimizing the conventional pMDI in order to create a better delivery system for patients, which does not include changing the drug particles themselves. Through the use of the modeling and simulation software COMSOL Multiphysics, we aim to develop an

accurate model that describes the fluid flow, diffusion through the air, and deposition of Salbutamol, a commonly used anti-asthma drug, in order to optimize insertion angle and spray cone angle and consequentially the flow rate. Ultimately, our focus is on minimizing drug deposition and maximizing the effective drug concentration to treat asthma and increase prognosis.

2.2 Design Objectives:

Our goal is to optimize the deposition of Salbutamol, a drug administered via inhaler that is used to prevent bronchospasm in patients with asthma, along the respiratory tract. We plan to use computational modeling to study the effect insertion angle, flow rate and injection velocity, and particle size have on the deposition of aerosol particles through the oral cavity, oropharynx, and laryngopharynx regions.

3. PROBLEM FORMULATION

3.1 Terms Defined:

Flow Rate: the steady inhalation rate of liquid particles without significant initial momentum.
Particle Density: the mass of the liquid particles injected by the inhaler. Particle mass will depend only on particle diameter as the density is assumed to remain constant at 1000 kg/m^3. Particle diameters range from 1μm to 30μm.
Particle Inlet Velocity: the velocity of the particles as they enter the oral cavity.

3.2 Schematics:

The geometry of the oral cavity, oropharynx, and laryngopharynx used in this study was adopted from Cheng et al., 1997 and simplified to reduce complexity in the calculations. This simplified geometry consists of two regions, the oral cavity and laryngeal-tracheal region, as shown in Figure 1.

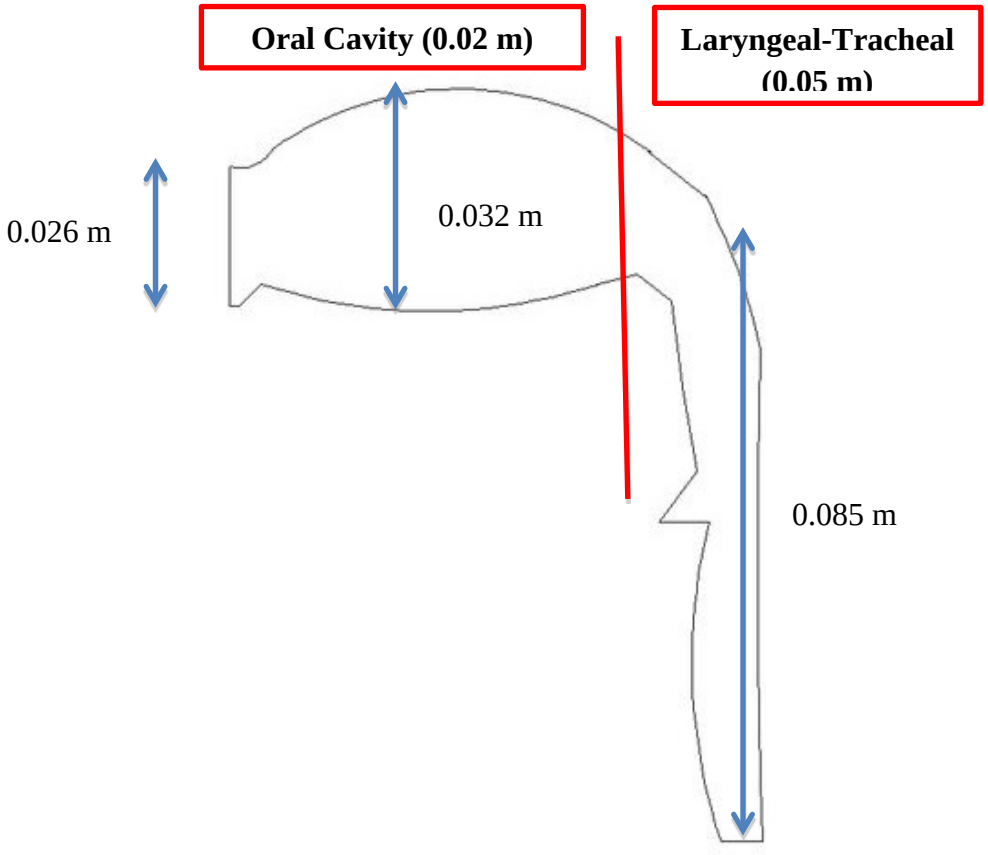

Figure 1: Schematic of the Oral Cavity, Oropharynx, and Laryngopharynx. The diagram was modified from Cheng et al (1997), and the dimensions are in meters. The simplified model is divided (by the red line) into two regions, the Oral Cavity and the Laryngeal-Tracheal, based on distance along the x-axis. Measurement lengths are shown in blue.

Using this geometry, along with approriate input parameters, the model's objective was to determine whether the spray particles would reach the end of the trachea and enter the bronchioles, or stick on the boundary. The region that had the greatest number of particles that stuck to the boundary was determined in COMSOL.

Mesh:

Based on the results obtained from Mesh Convergence Analysis (see Appendix B), the physics-controlled "Extra-Fine" mesh size was applied to the given geometry in Figure 1. The resulting mesh contained a total of 18322 elements (see Figure 2 below).

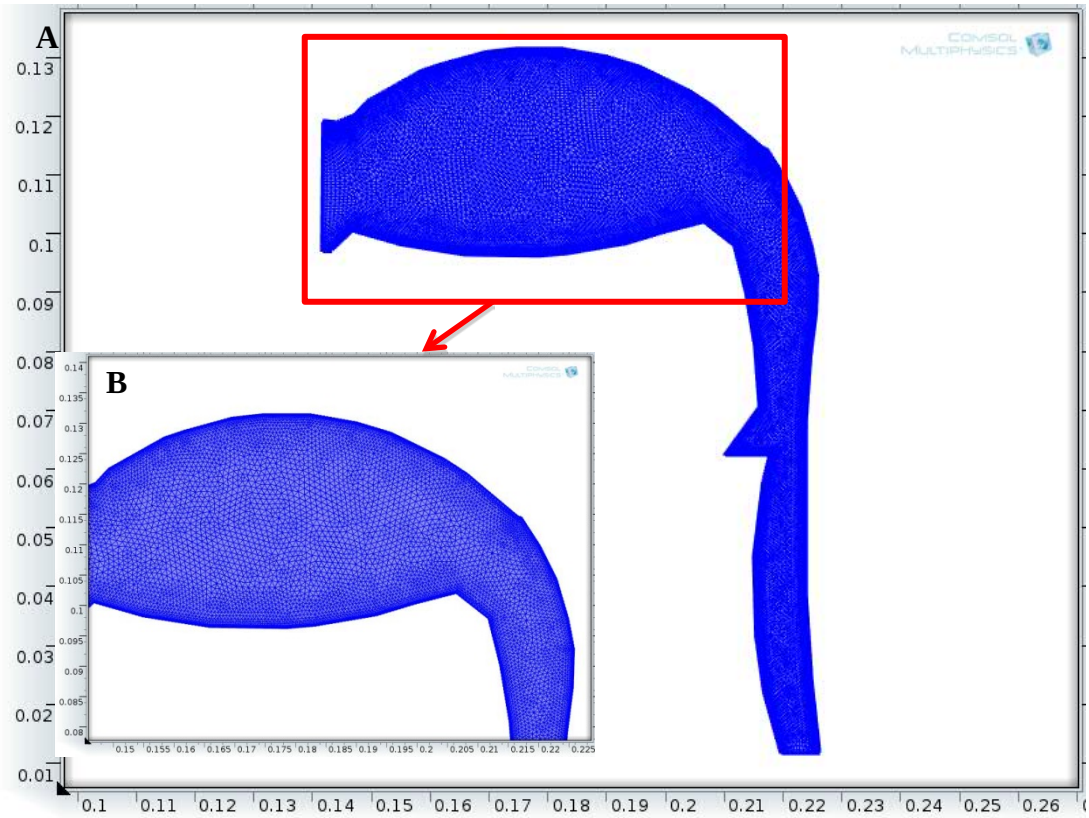

Figure 2: Final Mesh to be Used in COMSOL Modeling. (A) Unstructured Mesh of oral cavity and laryngeal-tracheal model from Figure 1. Extra fine, unstructured mesh was used, which contains 18322 triangular elements. **(B)** Closer view of the mesh distribution in the oral cavity and upper trachea.

3.3 Governing Equations:

In order to analyze the air flow in the oral cavity, the fluid was considered as a 2D turbulent flow using the low Reynolds number (LRN) $k-\omega$ model for transient conditions (Inthavong, K. et al., 2010). This model used the solutions of the conservation equations of mass and momentum. In addition, particle tracing was taken into account using Lagrangian Particle Tracing equations which are built into COMSOL as a module.

3.3.1 Turbulent Flow

Turbulence kinetic energy (k) equation:

$$\frac{\partial \overline{u_j}}{\partial x_j} = 0 \quad (1)$$

Momentum equation:

$$\frac{\partial \overline{u_j}}{\partial t} + \overline{u_j}\frac{\partial \overline{u_j}}{\partial x_j} = -\frac{1}{\rho}\frac{\partial \rho}{\partial x_j} + \frac{\partial}{\partial x_j}\left[\mu\left(\frac{\partial \overline{u_i}}{\partial x_j} + \frac{\partial \overline{u_j}}{\partial x_j} - \frac{2}{3}\delta_{ij}\frac{\partial \overline{u_k}}{\partial x_k}\right)\right] + \frac{\partial}{\partial x_j}\left(-\rho\overline{u'_i u_j'}\right) \quad (2)$$

Turbulence kinetic energy (k) equation:

$$\frac{\partial k}{\partial t} + \overline{u_j}\frac{\partial k}{\partial x_j} = \tau_{ij}\frac{\partial \overline{u_j}}{\partial x_j} - \beta * k\omega + \frac{\partial}{\partial x_j}\left[(\nu + \sigma_k \nu_k) + \frac{\partial k}{\partial x_j}\right] \quad (3)$$

Specific dissipation rate (ω) equation:

$$\frac{\partial \omega}{\partial t} + \overline{u_j}\frac{\partial \omega}{\partial x_j} = \alpha\frac{\omega}{k}\tau_{ij}\frac{\partial \overline{u_j}}{\partial x_j} - \beta\omega^2 + \frac{\partial}{\partial x_j}\left[(\nu + \sigma_\omega \nu_T) + \frac{\partial \omega}{\partial x_j}\right] \quad (4)$$

In contrast to the k-epsilon model, which solves for the dissipation or rate of destruction of turbulent kinetic energy, the k-omega model solves for the rate at which this dissipation happens. The basis of the governing equation of omega assumes the physics involved are those in the transport of a scalar in the fluid. By taking into consideration the processes of convection, diffusion, and destruction or dissipation, the omega equation is given by Equation 4 above.

The k-omega model's defect-layer structure is said to be consistent with measurements of turbulent boundary layers for all pressure gradients. The defect layer is defined as the near-wall boundary layer that includes the transition from where viscosity is negligible, to where it is significant. Also this model can be integrated through the viscous sublayer, without the presence of viscous damping functions. The viscous sublayer is defined as the thin fluid layer adjacent to the boundary where viscosity becomes significant enough to justify the no-slip boundary condition (Flierl et al, 2007).

3.3.2 Particle Tracing:

Lagrangian Particle Tracing:

$$m_p\frac{du_p}{dt} = \left[F_d(u_g - u_p)\right]m_p \quad (5)$$

$$F_d = \frac{\mu_g c_d R_{ep}}{24\rho_p {d_p}^2} \quad (6)$$

3.4 Flow Boundary Conditions

- No slip at the wall.
- Pharynx and larynx wall are rigid.
- Normal inlet velocity profile:
- $u = 1.2244 * u_m\left(\frac{R-r}{R}\right)^{\frac{1}{7}}$ (7)

    - Average velocity depends on the average inspiratory flow rates, which varies from approximately 30 L/min to 75 L/min (Zhang and Kleinstereuer, 2003)
    - Radius $R = 0.026$ m obtained from inlet dimensions.
    - $r = |\text{y coordinate} - (\text{center y coordinate at inlet})|$
- Pressure at outlet is assumed to be 0 Pa.
- Mucus layer is negligible.

3.5 Assumptions:

Fluid Flow

1. Air flow in oral cavity is modeled as Newtonian and incompressible fluid
2. Turbulent flow with low Reynolds number.

Particles

1. All particles are assumed to be spheres of the same size
2. Particles are stick with 100% efficiency once in contact with the cavity wall
3. The walls are permeable to drug
4. The geometry is 2D circular
5. All the particles that reach the end of the model will go into the lung

3.6 Input Parameters:

See Appendix A, Tables A1, A2, and A3 for the values used in the model.

4. RESULTS AND DISCUSSION

4.1 Results

4.1.1 Turbulent Flow

We ran our models for a range of flow rates from 30 L/min to 75 L/min, corresponding to inlet mean velocities of 0.9417 m/s to 2.354 m/s, particle inlet velocities from 5.1 m/s to 8.4 m/s, and varying particle diameters from 1 µm to 30 µm. As these different combinations of parameters were computed, the particle density remained constant at 1000 kg/m^3. The results showed that an optimal combination for minimal drug deposition was achieved at a flow rate of 30 L/min, with a spray velocity of 8.4 m/s for a particle size of 1 µm. Turbulent fluid flow through the oral cavity and laryngeal-tracheal region was based on the listed parameters in Appendix A, Table 1, and is illustrated in Figure 3.

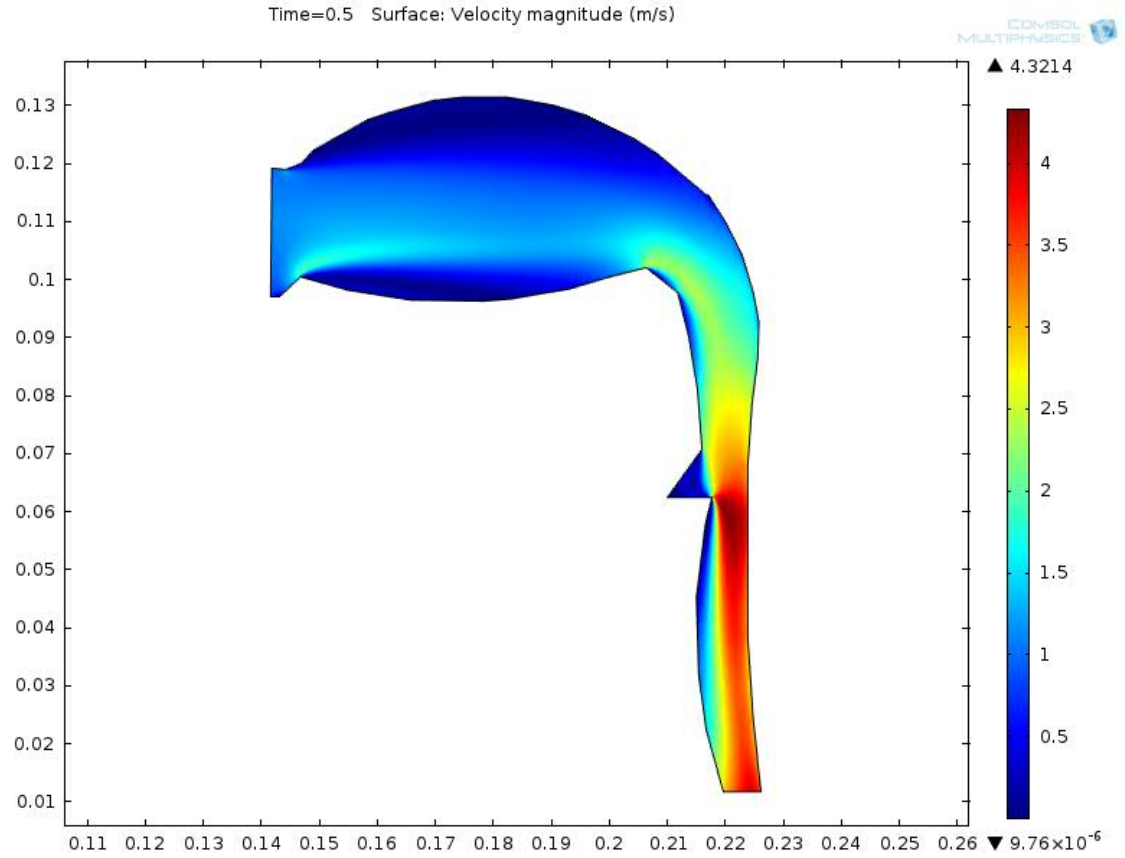

Figure 3: Turbulent velocity magnitude surface plot. This plot is obtained after 0.5 seconds with time step of 0.025 seconds. The particle with diameter of 1 µm is injected with 30 L/min flow rate and 8.4 m/s of spraying velocity.

Figure 3 shows that the air flow was smooth throughout the whole geometry, except at the esophagus. The high velocity magnitude at this location was due to the sharp corner of the geometry. Comparing to other typical turbulent model, there were minimal disturbances. This unique feature was due to the low Reynolds number obtaining from the range of low velocity. These Reynolds number confirmed that the flow, in fact, was in the transitional phase between

laminar and turbulent. However, it is reasonable to consider this phenomenon as the 2D turbulent flow by using low Reynolds number $k-\omega$ turbulent flow module in the computation (Inthavong, K., et al, 2010)

4.1.2 Particle Tracing

After being released at time zero, the particles followed the turbulent flow through the oral cavity. They then traveled down the laryngeal-tracheal region, and eventually reached the lungs. During this process, the particles that touched the boundaries were captured, due to our assumption of one hundred percent sticking efficiency. Additionally, percent deposition is defined as the ratio of wall-attached particles total particles released by the inhaler. Figure 4 shows that percent deposition increased and then remained constant after approximately 0.1 seconds. The shoot-off rate depended highly on the flow-rate and spray velocity.

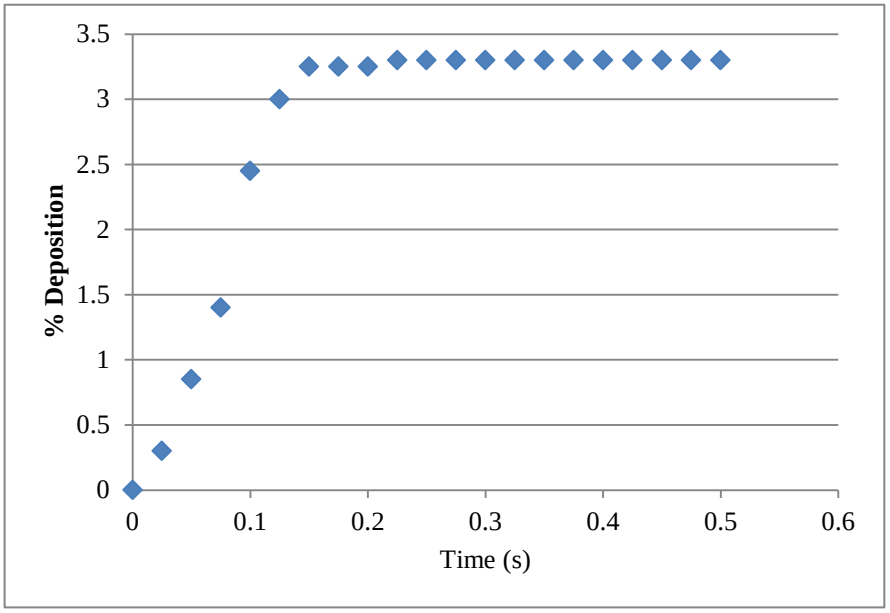

Figure 4: Deposition Percentage over time. Shown is the percent deposition of the particles, which have diameters of 1 µm, on the boundary layer versus time for flow rate of 30 L/min and a particle velocity at the inlet of 8.4 m/s.

Figure 4 shows that after approximately 0.15 seconds, the number of particles found at the geometry's boundary did not increase, but stabilized instead. This shows that, without layering of particles, the main particle sticking only occurs within the first 0.2 seconds. Figure 5 provides a better visualization of the drug deposition, with the dots representing drug particles.

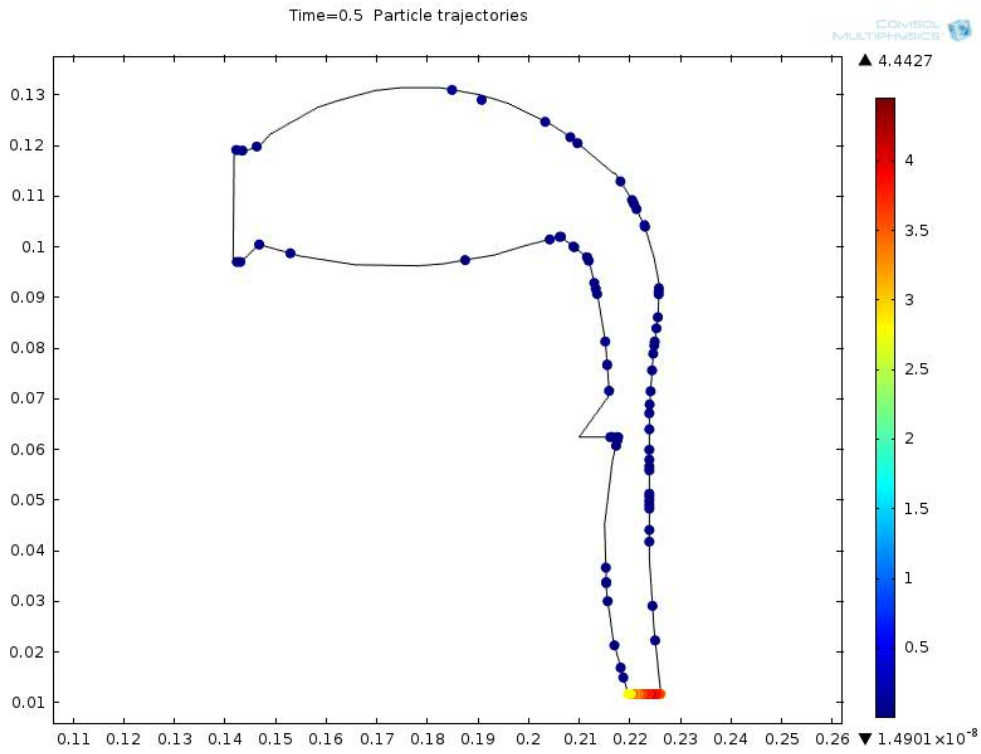

Figure 5: Drug deposition surface plot. This is a plot of the final particle placements after 0.5 seconds with time step of 0.025 seconds. The particles, with diameters of 1 μm, are injected with a 30 L/min flow rate and an 8.4 m/s spraying velocity.

Figure 5 provides valuable information about the specific location of each drug particle, either on the oral cavity boundary or laryngeal-tracheal boundary. For the purpose of simplifying the results analysis, it is assumed that if the drug's horizontal location is smaller than 0.2 μm while its vertical location is smaller than 0.0107 μm (since it is incorrect to count the drugs found at the end of the trachea), the particle located in the oral cavity region, otherwise it is located in the laryngeal-tracheal region. Relying on the drug deposition profile, the region with the most deposition could be determined. However, this conclusion depends directly on particle size, flow rate, and particle velocity at inlet (data not shown).

4.3 Accuracy Check

To validate our model, Cheng et al (2001) was used as a comparison. Using the range of diameters provided by Cheng et al, the median diameter of 2.33μm was chosen for the model particles.

Although there is a spacer present in Cheng et al's model, the data could still be used as for validation, and the geometry did not have to be accommodated. Cheng's group starts to model deposition from the start of a spacer with a diameter of 0.026m. The model proposed here, on the other hand, models deposition starting from the mouth. However, because the mouth is over the mouthpiece, it can be assumed that the mouth has the same diameter as the spacer and thus a diameter of 0.026m is valid.

Cheng's research shows that there is a 52% deposition in the apparatus they used, so it may be assumed that the remainder is deposited into the oral pathway. Consequently, when starting off with 2000 particles from the inhaler, 960 particles reach the mouth, which is where the proposed model begins. The model initially released 960 particles, run over a period of 0.5 seconds with a time step of 0.25. Using the global evaluation to analyze how many particles stick over time, we found that 54 particles stick overall in the geometry for one inhalation of breath.

As a result, the model computed a deposition of 2.7%, which confirms Chen et al's 1.1% deposition in the oral airway. Although this value is more than double the percentage that Cheng's group determined, the discrepancy is most likely due to the difference in dimension. Cheng, et al's model was in 3D, whereas the model shown here was 2D, which causes an increase in percent deposition. There is more room for particles to travel in 3D, and hence less stickiness, because the velocity vector in a 3D model gets broken up into 3 components, while a 2D model consists of 2 components.

4.4 Sensitivity Analysis

Our sensitivity analysis focused on the effects of four parameters on drug deposition: flow rate, insertion angle, drug diameter, and particle velocity at the inlet. Our goal for this analysis is to determine the set of optimal parameters that have the lowest percent deposition on the boundary in both the oral cavity and the laryngeal-tracheal region. Parameter values were found in Hochrainer et al (2005) and Inthavong et al (2010), then modified to better fit the model. First, four inlet flow rates (30, 50, 60, and 75 L/min), were used to calculate the mean velocities listed in Table 3 (Appendix A). Next, these results were used to obtain the velocity profile at the inlet for 2D-turbulent flow by using Equation (7). In addition, a range of spray velocities was tested. Particle mass was varied by changing the diameter while keeping the density constant at 1000 kg/m^3. Insertion angle was varied by changing the x and y components of the inlet velocity for particles.

Figure 6 and 7 show the sensitivity analysis for the model. 3-D bar graphs were used to determine the effect of two unique parameters on particle deposition. In Figure 6, percent deposition is found for different combinations of particle inlet velocity, drug diameter, and average velocity of turbulent flow to determine which the optimal set is. From A to B, the flow rates are 30 L/min (0.9417 m/s) and 50 L/min (1.5695 m/s), respectively. In each plot, from front to back, there is an increase in particle diameter; from left to right, particle inlet velocity is higher. Deposition percentage will then be compared in each direction of all the 3-D bar graphs. In order to provide a better visualization, taking the data from Figure 6-A, Figure 6-C is used to determine the change in particle deposition as particle inlet velocity increases. Similarly, Figure 6-C shows the change in percent of deposition for different drug sizes.

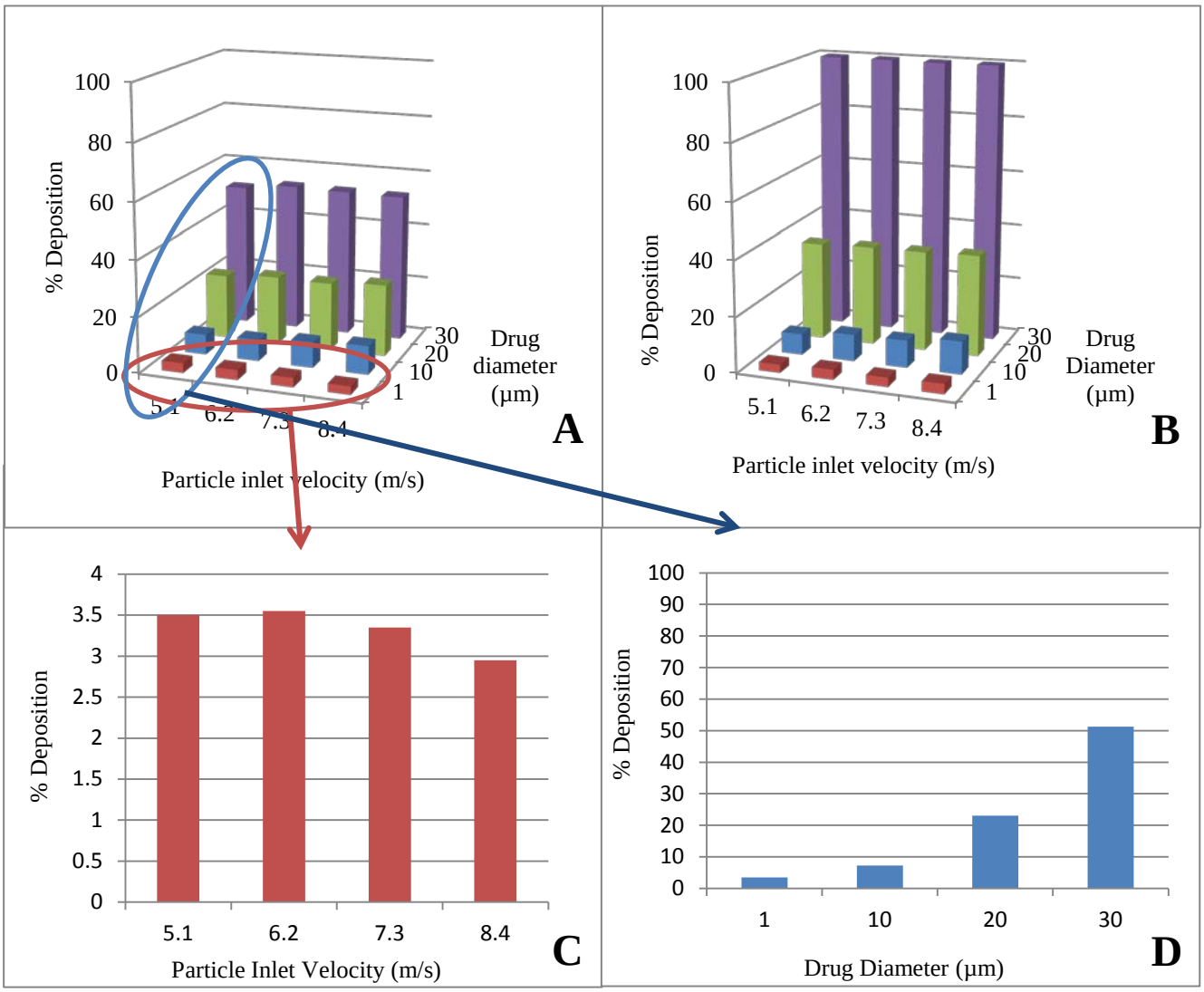

Figure 6: Sensitivity analysis of particle inlet velocity and drug diameter on particle deposition. The range of drug diameters and particle inlet velocities are considered for flow rates (and corresponding mean velocities) of (A) 30 L/min (0.9417 m/s) and (B) 50 L/min (1.5695 m/s). Using the data from (A), percent deposition is plotted against the change in particle inlet velocity in (C) and against drug diameter in (D). As the drug diameter increased, higher particle deposition was observed. As particle inlet velocity increased, there was no significant difference between the four data sets. As flow rates increased, increased particle diameter resulted in fewer particles reaching the bottom of the trachea.

Figure 6 shows that as the drug diameter increased, the percent deposition of drug also increased. However, the deposition was not significantly affected by the particle velocity at the inlet. Comparing all four plots, lesser deposition was observed as the flow rate decreased. These results are realistic because drug movement is greatly affected by momentum, and as particle mass increases, momentum and also the probability of coming into contact with the boundary increases, thus leading to an increase in the amount of drug that sticks to the boundary.

In conclusion, the least deposition (2.95%) was found at a flow rate of 30 L/min with a 5.1 m/s spray velocity and a particle size of 1 μm. Next, the optimal combination for each insertion angle was tested with changing flow rate for the particle diameter of 2.33 μm (see Figure 7 on next page for results). This value was chosen because it is the diameter of salbutamol, the chosen drug to be tested (Cheng et al, 2001). Figures 8-A and 8-B show the difference in drug deposition between the flow rates of 30 L/min and 50 L/min. In each plot, from front to back, there is an increase in insertion angle while from left to right, particle inlet velocity is higher. With the purpose of providing a better visualization, adapting the data from Figure 7-A, Figure 7-C is used to determine the change in particle deposition as particle inlet velocity increases. Similarly, Figure 7-D shows the change in percent of deposition for different insertion angles.

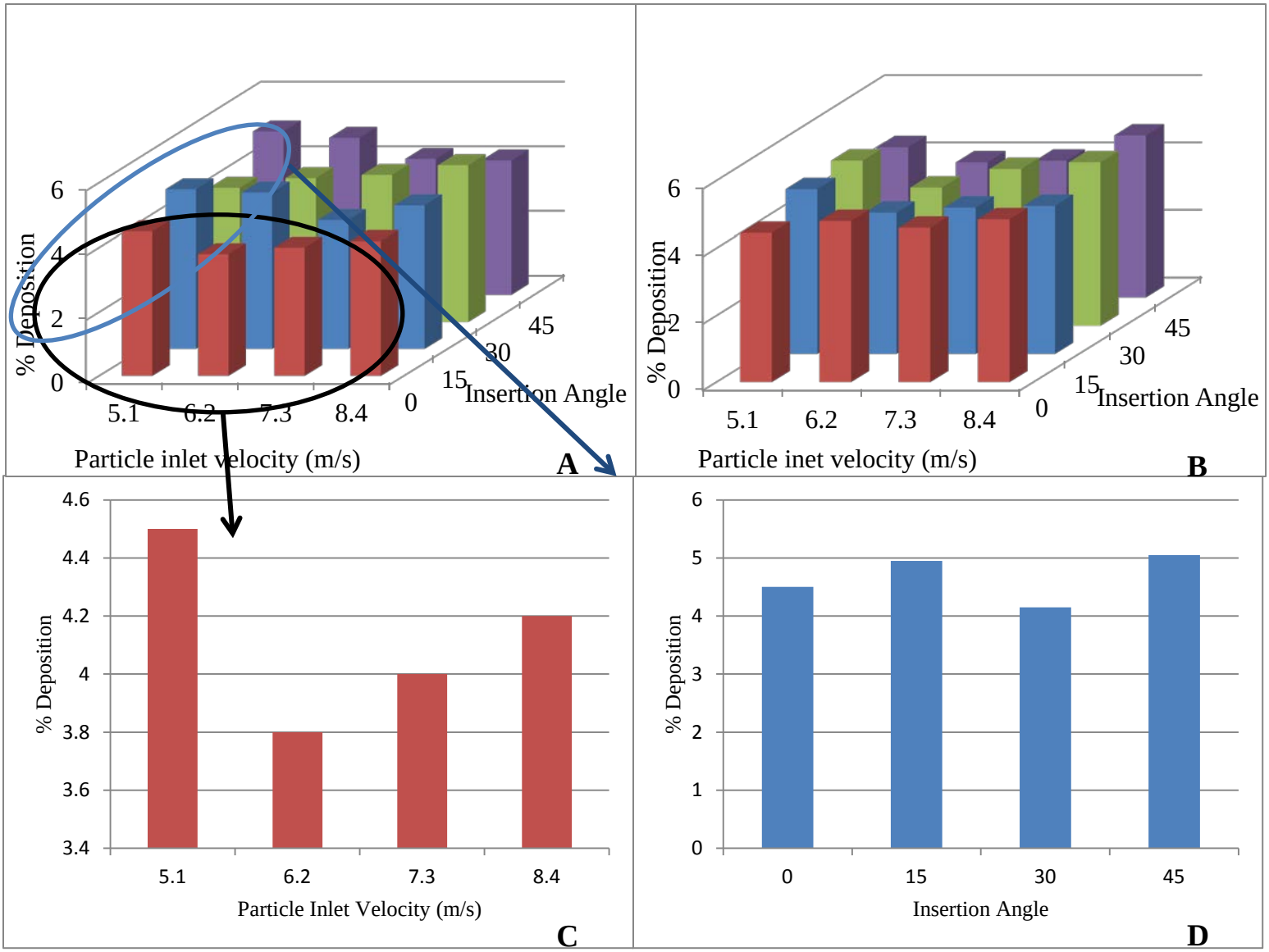

Figure 7: Sensitivity analysis of particle inlet velocity and insertion angle on particle deposition for a drug diameter of 2.33 µm. The range of drug insertion angles and particle inlet velocities are considered for flow rates (and corresponding mean velocities) of (A) 30 L/min (0.9417 m/s), (B) 50 L/min (1.5695 m/s). Using the data from (A), percent of deposition is plotted against the change in particle inlet velocity in (C) and against insertion angle in (D). As particle inlet velocity increased, there is less than 1% difference between the four data sets. As the insertion angle increased, there is also less than 1% difference in the deposition. Additionally, the percent deposition did not vary significantly when the flow rates were increased as well.

Figure 7 shows that the particle inlet velocity, insertion angle, and flow rate did not have any noteworthy effects on percent of drug found on the boundary. These results could arise from several sources of error. First, the isotropic turbulence, k-ω model could be an invalid approximation because according to Delvadia et al (2012), this model was thought to overestimate the aerosol deposition. Instead, this paper considered the assumption of anisotropic near-wall turbulence. Second, we did not consider the presence of the tongue in the oral cavity.

In this case, the tongue could play an important role in preventing the drugs from sticking on the boundary of the oral cavity as the insertion angles of the inhaler are varied.

5. CONCLUSIONS AND DESIGN RECOMMENDATION

5.1 Conclusion

From our sensitivity analysis, we concluded that there is a significant dependence of drug deposition on particle momentum. For each flow rate tested (30-75 L/min), drug deposition increased notably for increasing particle size. This shows that inertial impaction is a main cause of deposition, a finding that has been confirmed in other studies (Cheng, et al, 2010). Particle velocity begins to influence particle deposition for particles $\geq$10um, with higher particle velocities resulting in slightly higher deposition, which is expected since increasing velocity also increases particle momentum. If effective administration of drug is defined as having less than 10% particle deposition in the upper airway tract, then drugs with particle sizes of around 1µm are considered effective regardless of breathing flow rate of the patient and velocity of particles from the inhaler.

5.2 Design Constraints

While our design offered a thorough analysis of the delivery of salbutamol via inhaler, it is constrained to only model this one drug. In order to extend the application more accurately to other drugs, parameters such as particle density, particle diameter, and number of particles per release should be adjusted accordingly. Drugs with higher density may result in more deposition and, as our preliminary results indicate, drugs with larger particle sizes are influenced more greatly by particle velocity from the inhaler nozzle.

In addition, our model only applies for a 2D situation with a mouth opening of 1.3cm radius. Geometries of the oral cavity and laryngeal-trachea region vary from person to person, which may affect the amount of deposition as well as local velocity fields for normal breathing. Generally, adults may have a larger trachea diameter than children and thus would have less particle deposition as well as lower flow velocities in this region. The surface area available for particle deposition would likely be significantly different for a 3D model, so while the current 2-dimentional model is suitable in determining relative differences in particle deposition, it still poses a significant constraint to our design.

5.3 Design Recommendations and Future Work

Based on our study we determined that the least drug deposition for moderately sized drug particles of around 1 to 10 µm is achieved at a flow rate of approximately 30 L/min, a typical inhalation rate for a resting individual (Zhang et. al, 2004), and a particle inlet velocity of 5.1 m/s, which falls in the range of velocities for pMDIs (Hochrainer et. al, 2005). Because infants and children generally have a greater flow rate than adults, in using an inhaler for a 1-10µm particle drug such as salbutamol, an insertion angle of 0° (directly into the mouth) is suggested. For larger drug particles, we recommend that the spray velocity of the inhaler be reduced, perhaps by increasing the cross sectional area of the opening of the inhaler. Alternatively, for

drugs that tend to disperse as larger particles, the spray mechanism of the inhaler can be customized to reduce their size to be closer to 1μm, at which point the particle velocity has no significant effect on drug deposition and would no longer need to be taken into account in the design of the pMDI.

Based on our design constraints, these recommendations only apply to a restricted population with upper airway anatomies that are similar to the geometry used in this study. Exploring more complex geometries for specific scenarios is one potential avenue for future work.

5.4 Implications and Relevance

In finding optimal values for the inhaler insertion angle for a variety of flow rates and particle velocities, we can apply the implications of our study to have significant impact on the future of pMDI use. Because children typically breathe with higher flow rates than adults, custom pMDIs can be made that encase the drug in smaller particles, thereby decreasing deposition. For even more precise inhalers for patients with unusual breathing flow rates, pMDIs can also be made with custom cross sectional areas of the opening so that a particular initial particle velocity can be achieved.

Because our sensitivity analysis includes data on a range of particle diameters, our study has found preliminary data for other drugs of different sizes as well. These results show us that the fractional deposition of drug in the upper airway tract increases significantly for larger particle sizes. The implications of these results may spark further research into studying the specifics of drug deposition for larger particles, such as location of particle deposition and the effects of different turbulent flow models, focusing attention to the drugs in which upper airway deposition poses the greatest problem, so the most improvement can be made.

Our study focused on salbutamol, an anti-asthmatic bronchodilator. However, the results of our study are not only limited within the context of treating asthma. Salbutamol’s widespread use in treating bronchitis, emphysema, and other lung diseases allows our model to also have relevance to patients with these conditions as well.

APPENDIX A: SOLUTION STRATEGY

The input parameters and units used are shown in Table A1, A 2, and A3.

Table A1. Constant Input Parameters. These values do not vary in the experimental process. Shown below are the value, unit, and source of each parameter, as well the definition of each value in relation to this project.

Parameter	Definition	Value	Units	Source
ρ_g	Fluid density at 298 K	1.1839	kg/m^3	(Engineering Toolbox)
μ_g	Fluid Dynamic viscosity at 298 K	1.9632e-5	Pa.s	(Engineering Toolbox)
$u_{g,x}$	Initial velocity field of fluid flow	0	m/s	(Longest, P., et al, 2008)
$u_{g,y}$		0	m/s	(Longest, P., et al, 2008)
p_g	Outlet pressure	0	Pa	(Longest, P., et al, 2008)
ρ_p	Particle density	1000	kg/m^3	(Longest, P., et al, 2008)
d_p	Particle diameter	2.33e-6	m	(Cheng, Y. S., et al, 2001)
z	Charge number	0		(Cheng, Y. S., et al, 2001)
K	Turbulent kinetic energy	0.05	m^2/s^2	(Inthavong, K. et al., 2010)
$g_{p,x}$	Gravity vector of particle tracing for fluid flow	0	m/s	(Inthavong, K. et al., 2010)
$g_{p,y}$		-9.81	m/s	
C_μ	Turbulence constant	0.09		(Inthavong, K. et al., 2010)
α	Turbulence constant	0.555		(Inthavong, K. et al., 2010)
β	Turbulence constant	0.8333		(Inthavong, K. et al., 2010)
β	Turbulence constant	1		(Inthavong, K. et al., 2010)
σ_k	Turbulence constant	0.5		(Inthavong, K. et al., 2010)
σ_ω	Turbulence constant	0.5		(Inthavong, K. et al., 2010)

Table A2. Varying Input Parameters. These parameters varied during sensitivity analysis and validation, but were constant during each COMSOL run. The range of values used is given. The units and the definition of each value in relation to this project are also provided. These values were obtained from Hochrainer, D., et al, 2005 and Inthavong, K., et al, 2010.

Parameter	Definition	Range of Values	Units
d_p	Particle Diameter	1, 10, 20, 30	μm
Q	Flow Rate	30, 50, 60, 75	L/min
u_o	Particle Velocity at Inlet	5.1, 6.2, 7.3, 8.4	m/s

Table A3. Varying Mean Velocities and Flow Rates at the Inlet. Shown are different mean velocities of turbulent flow at the inlet with given flow rates and the radius of the inlet at 0.013 μm. The velocities were calculated using equation (7).

#	Average Flow rate (L/min)	Mean velocity (m/s)
1	30	0.9417
2	50	1.5695
3	60	1.8834
4	75	2.3543

Table A4. Particle Velocity at Inlet as a function of Insertion Angles. Depending on the mean velocity, the velocity at the inlet in the x and y directions was determined. This methodology was obtained from Inthavong, K., et al, 2010.

Insertion Angle (^{o})	Particle Velocity at Inlet (m/s)				
		5.1	6.2	7.3	8.4
0	u_x	5.1	6.2	7.3	8.4
	u_y	0	0	0	0
15	u_x	$5.1\cos(\pi/12)$	$6.2\cos(\pi/12)$	$7.3\cos(\pi/12)$	$8.4\cos(\pi/12)$
	u_y	$5.1\sin(\pi/12)$	$6.2\sin(\pi/12)$	$7.3\sin(\pi/12)$	$8.4\sin(\pi/12)$
30	u_x	$5.1\cos(\pi/6)$	$6.2\cos(\pi/6)$	$7.3\cos(\pi/6)$	$8.4\cos(\pi/6)$
	u_y	$5.1\sin(\pi/6)$	$6.2\sin(\pi/6)$	$7.3\sin(\pi/6)$	$8.4\sin(\pi/6)$
45	u_x	$5.1\cos(\pi/4)$	$6.2\cos(\pi/4)$	$7.3\cos(\pi/4)$	$8.4\cos(\pi/4)$
	u_y	$5.1\sin(\pi/4)$	$6.2\sin(\pi/4)$	$7.3\sin(\pi/4)$	$8.4\sin(\pi/4)$

APPENDIX B: MESH CONVERGENCE ANALYSIS

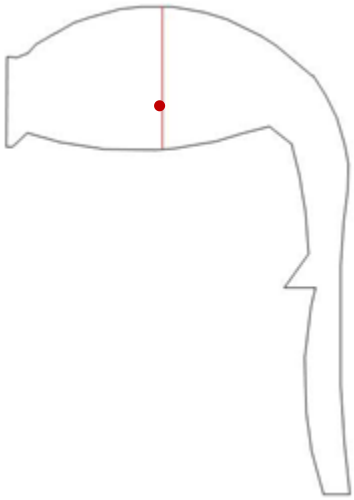

Figure B1: Schematic of oral cavity and laryngeal-trachea regions. The red line located in the middle of the cavity is where the average velocity is taken for the mesh convergence analysis.

The mesh convergence analysis was performed based on the average value of the velocity for a cut line 2D from (0.18, 0.096) to (0.18, 0.132) shown in Figure B1. The velocity was evaluated at seven different mesh sizes. Figure B2 shows that velocity profiles for different types of meshing appears to begin to overlap at the "Extra Fine" element size at our chosen point (18322 elements). As a result, the particle velocity is independent of our mesh after 18322 elements. In Figure B3, we can also see that the change in velocity is negligible for mesh sizes smaller or equal to that of the “Extra fine” element size, confirming our qualitative reasoning.

Mesh convergence was also performed on the particle trajectory (see Figure B4). It was found that the coarse and extremely coarse meshes are the least accurate for modeling. Once the extra fine or extreme fine meshes are used, the trajectories are more detailed (not shown) and the percent of drug deposition converges. Taking this data into account along with our analysis on particle velocity, we plan on using 18322 elements in our final design, corresponding to the Extra Fine mesh size.

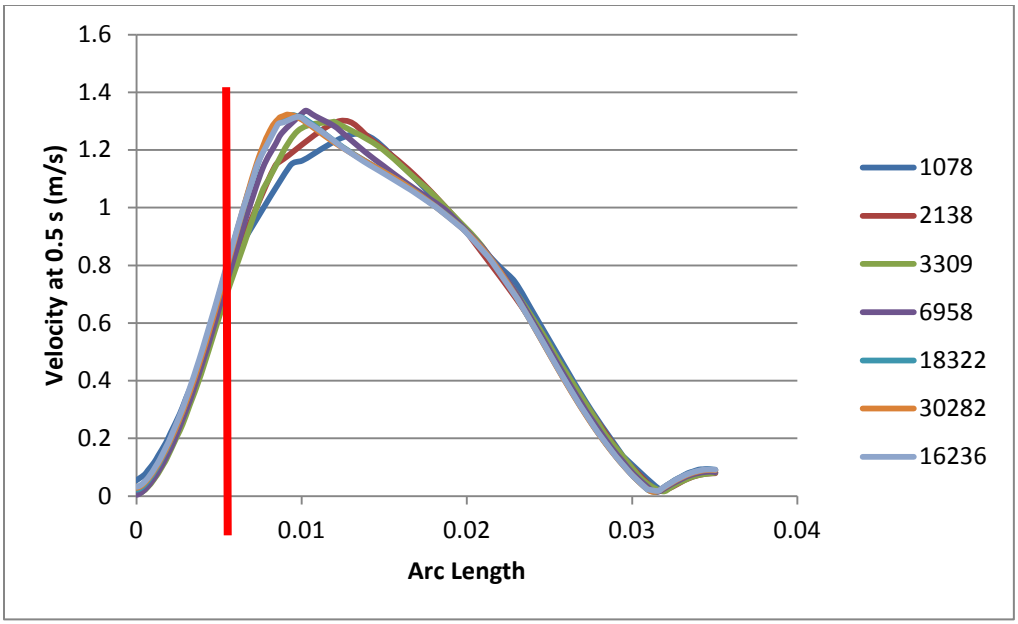

Figure B2: Velocity Profile for Cut Line 2D from (0.18, 0.096) to (0.18, 0.132) for different types of meshing**.** Average velocity profile at 0.5 seconds for seven different types of meshing at point x = 0.006 m (illustrated by red lines).

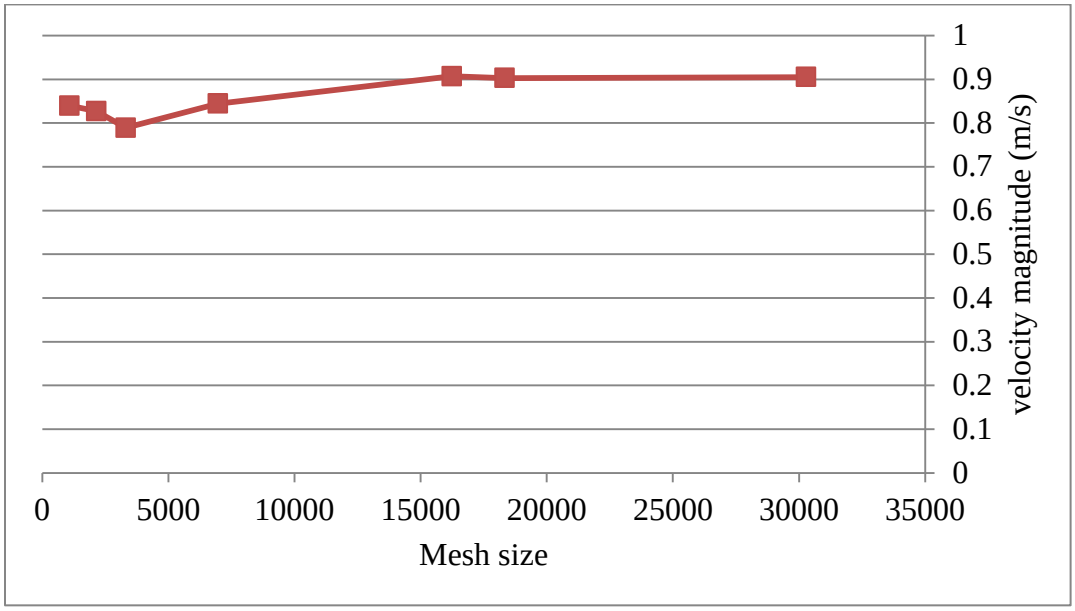

Figure B3: Mesh convergence analysis of oral cavity and laryngeal-trachea regions based on the average velocity profile at point x = 0.006 in the cutline 2D from (0.18, 0.096) to (0.18, 0.132) (see Figure 10 for point). Figure 12 shows that after number of elements of 18322, the velocity magnitude at point x = 0.006 is converged.

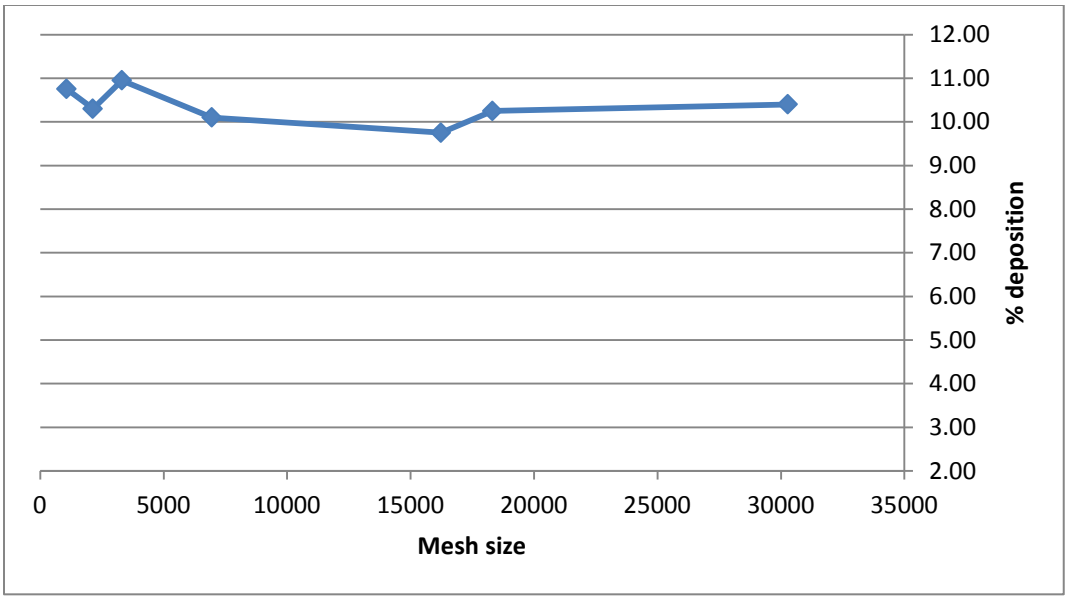

Figure B4: Percent of drug deposition on oral cavity and laryngeal-trachea regions for different number of mesh elements. Figure 13 shows that after number of elements of 18322, the deposition percentage remains constant. This confirms the independence of the result on mesh size after 18322 elements.

APPENDIX C: SOFTWARE IMPLEMENTATION

To ensure the blunt parabolic nature of our particle inlet velocity, the velocity profile equation (Eqn. 7) was plotted in MATLAB by implementing the code shown in Figures C1 and C2. The resulting profile is shown in Figure C3.

C1

```
%particle positions:
y=[0.119104771
0.119115214
0.119125658
0.11906822
.
.
.
0.09708463
0.097095473
0.097106315
0.097117158
0.097128001];

%define flow rate:
f = 30; %L/min
radius = 0.011; %m
for i=1:size(y)
vel = feval('velprof',y(i),f,radius);
plot(y(i) - min(y),vel)
hold on
end
axis([.095-min(y) .12-min(y) 0 2])
xlabel('Distance from bottom of mouth
opening (m)')
ylabel('Velocity (m/s)')
, from flow rate:
um = f/60*0.001/(pi()*rad^2);
vel = 1.2244*um*((rad-r)/rad)^(1/7);
```

C2

```
%inlet velocity profile
function vel = velprof(y,f,rad)
y_center=.108083; %average of minimum and
maximum particle pos'n
r = abs(y-y_center);
%calculate mean velocity, um, from flow rate:
um = f/60*0.001/(pi()*rad^2);
vel = 1.2244*um*((rad-r)/rad)^(1/7);
```

C3

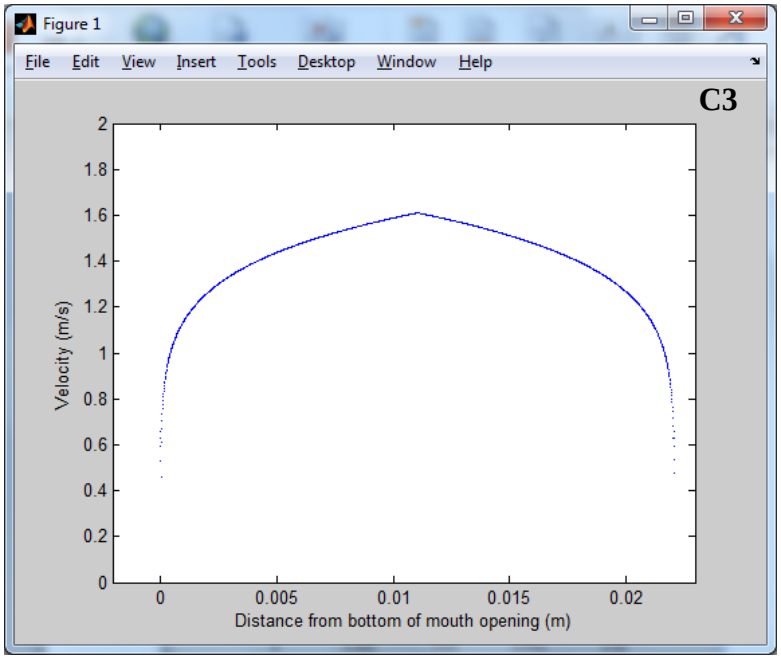

Figure C. Velocity of drug particles at the inlet models a blunt parabolic profile. (C1) MATLAB programming language was used to plot the particle inlet velocity equation for a breathing flow rate of 30 L/min. (C2) Velocity profile equation was called as a separate function for flexible programming. (C3) Results were plotted as a function of distance from the bottom of the mouth opening.

APPENDIX D: REFERENCES

1- American Academy of Allergy Asthma and Immunology (2013) Asthma Statistics. *http://www.aaaai.org*. Retrieved on April 8th, 2013. http://www.aaaai.org/about-the-aaaai/newsroom/asthma-statistics.aspx

2- Virchow, J. C., Crompton, G. K., Dal Negro, R., Pedersen, S., Magnan, A., Seidenberg, J., & Barnes, P. J. (2008). Importance of inhaler devices in the management of airway disease. *Respiratory medicine*, *102*(1), 10.

3- Vathenen, A. S., Britton, J. R., Ebden, P., Cookson, J. B., Wharrad, H. J., & Tattersfield, A. E. (1988). High-dose inhaled albuterol in severe chronic airflow limitation. *American Journal of Respiratory and Critical Care Medicine*, *138*(4), 850-855.

4- Drug Information Online (2013) Salbutamol. http://www.drugs.com . Retrieved on April 8th, 2013. http://www.drugs.com/cons/salbutamol.html

5- Kay, A. B. (2008) Allergy and Allergic Diseases. Blackwell. 2008.

6- Crosland, B. M., Johnson, M. R., and Matida, E. A. (2009) Characterization of the Spray Velocities from a Pressurized Metered-Dose Inhaler. *Journal of Aerosol Medicine and Pulmonary Drug Delivery*, *22*(2), 85-97.

7- Ehtezazi, T., et al. (2009), The Interaction Between the Oropharyngeal Geometry and Aerosols via Pressurised Metered Dose Inhalers. *Pharmaceutical Research*, 27 (1), 175-186.

8- Svartengren,K. et al.(1996) Oropharyngeal Deposition of 3.5 μm Particles Inhaled through an Elongated Mouthpiece. *European Respiratory Journal*, 9:1556-1559.

9- Cheng, K. H., Cheng, Y.S., Yeh, H. C., Swift D. L. (1997) Measurements of airways dimensions and calculations of mass transfer characteristics of the human oral passage. *Europe PubMed Central*, *119*(4), 476-482.

10- Zhang, Z. and Kleinstereuer, C (2003) Species heat and mass transfer in a human upper airway model. *International Journal of Heat and Mass Transfer*, *46*(25), 4755-4768.

11- "Air- Absolute and Kinematic Viscosity." *The Engineering ToolBox*. N.p., n.d. Web. 7 Mar. 2013. <http://www.engineeringtoolbox.com/air-absolute-kinematic-viscosity-d_601.html>.

12- Anthony, T.R. and Flynn, M.R. CFD Model for a 3-D Inhaling Mannequin: Verification and Validation.

13- Inthavong, K. et al. (2010) Micron particle deposition in a tracheobronchial airway model under different breathing conditions. *Medical Engineering & Physics*, *32(10),* 1198-1212.

14- "Healthcare Professionals." *Alvesco*. N.p., n.d. Web. 7 Mar. 2013. <http://www.alvesco.us/hcp/healthcare-professionals.html>.

15- Inthavong K., Tian, Z. F., Tu X. J, Yang, W., Xue, C., (2008). Optimising nasal spray parameters for efficient drug deliver using computational fluid dynamics. *Computers in Biology and Medicine* 38: 713-726

16- P. Worth Longest, Michael Hindle, Suparna Das Choudhuri, Jinxiang Xi, 2008. Comparison of ambient and spray aerosol deposition in a standard induction port and more realistic mouth–throat geometry. *Journal of Aerosol Science* 39:572-59

17- Cheng, Y.-S. et al. (1999). Particle Deposition in a Cast of Human Oral Airways. *Aerosol Science and Technology* 31:4, 286-300

18- Cheng, Y.S., Fu, C.S., Yazzie, D., and Zhou, Y. (2001). Respiratory Deposition Patterns of Salbutamol pMDI with CFC and HFA-134a Formulations in a Human Airway Replica. *Journal of Aerosol Medicine* 14(2), 255-266.
19- Xi, J., and Longest, P.W. (2007). Transport and Deposition of Micro-Aerosols in Realistic and Simplified Models of the Oral Airway. *Annals of Biomedical Enginering*, (35)4, 560-581.
20- Hoe, S., Traini, D., Chan, H.K., and Young, P. (2009). The Influence of Flow Rate on the Aerosol Deposition Profile and Electrostatic Charge of Single and Combination Metered Dose Inhalers. *Pharmaceutical Research*, 26(12), 2639-2646.
21- Hochrainer, D., Holz, H., Kreher, C., Scaffidi, L., Spallek, M., and Wachtel, H. (2005). Comparison of the Aerosol Velocity and Spray Duration of Respimat® Soft Mist™ Inhaler and Pressurized Metered Dose Inhalers. *Journal of Aerosol Medicine*, 18(3), 273-282.
22- Zhang, Z. and Kleinstreuer, C. (2004). Airflow Structures and Nano-Particle Deposition in a Human Upper Airway Model. *Journal of Computational Physics*, 198(1), 178-210.
23- Flierl, G. and Ferrari, R. (2007) Chapter 20. Boundary layer turbulence. *Turbulence in the Ocean and Atmosphere CourseNotes.* Retrieved on May 1st, 2013. <http://ocw.mit.edu/courses/earth-atmospheric-and-planetary-sciences/12-820-turbulence-in-the-ocean-and-atmosphere-spring-2007/lecture-notes/ch20.pdf>